

PHYSIQUE DE LA MATIÈRE EN GRAINS *PHYSICS OF GRANULAR MEDIA*

Evolution and shapes of dunes

Hans J. Herrmann^{a,b}

^a ESPCI, PMMH, 10, rue Vauquelin, 75231 Paris, France

^b Institute for Computer Applications 1, University of Stuttgart, Pfaffenwaldring 27, 70569 Stuttgart, Germany

Received 4 October 2001; accepted 11 December 2001

Note presented by Guy Laval.

Abstract The motion of dunes and their morphology is a fascinating, largely unexplored subject. Already the barchan, the simplest moving dune, poses many questions. I will present some results of field-measurements on desert and coastal dunes. Then I will present a model which consists of three coupled equations of motion for the topography, the shear stress of the wind and the sand flux. These evolution equations are verified on the experimental data and new possibilities of simulations of dunes are put in perspective. *To cite this article: H.J. Herrmann, C. R. Physique 3 (2002) 197–206.* © 2002 Académie des sciences/Éditions scientifiques et médicales Elsevier SAS

dunes / saltation / field measurements / modelization

Evolution et formes des dunes

Résumé Les mouvements des dunes et leur morphologie est un sujet fascinant et peu exploré. Déjà la barchane, la dune mobile la plus simple, pose des nombreuses questions. Je présente quelques résultats des mesures sur les terrains pour des dunes côtières et désertiques. Ensuite je présenterai un modèle consistant de trois équations de mouvement couplées, une pour la topographie, une pour la force de cisaillement du vent et la troisième pour l'écoulement de sable à la surface. Ces équations sont validées auprès des données expérimentales et des perspectives nouvelles pour la simulation des dunes sont présentées. *Pour citer cet article: H.J. Herrmann, C. R. Physique 3 (2002) 197–206.* © 2002 Académie des sciences/Éditions scientifiques et médicales Elsevier SAS

dunes / saltation / field measurements / modelization

1. Introduction

We all admire the beautiful wave-like shapes of the dunes in the desert. Sand dunes develop wherever sand is exposed to an agitating medium (air, water, ...) that lifts grains from the ground and entrains them into a surface flow. The diverse conditions of wind and sand supply in different regions on Earth give rise to a large variety of different shapes of aeolian dunes [1–3]. Moreover, dunes have been found on the sea-bottom and even on Mars. Despite the long history of the subject, the underlying physical

E-mail address: hans@ica1.uni-stuttgart.de (H.J. Herrmann).



Figure 1. Barchan dunes near Laâyoune, Morocco. The dune in the front, on the left side was measured in detail during our field trip in May 1999, see [14].

mechanisms of dune formation are still not very well understood. How are aerodynamics (hydrodynamics) and the particular properties of granular matter acting together to create dunes? How is the shape of a dune maintained when it moves and matures? What determines the size of dunes? Due to the fact that neither now nor in the near future will we be able to simulate dunes on the grain scale (an average barchan comprises 10^{15} grains), we concentrate in the following on an effective continuum model that can be applied to sand dunes or other geomorphological problems on a large scale. Due to the highly complicated physical processes involved (saltation, turbulent wind) and the wide range of length and time scales to be covered—from the dynamics of single sand grains, the formation of ripples, to the genesis and migration of dune fields, the time and length scales span over more than seven orders of magnitude—the derivation of the model will not be given here. We will instead after reviewing our experimental measurements present the basic elements of the model and finally compare the two.

The simplest and best known type of dune is the barchan dune shown in Fig. 1, shaped in a crescent, which occurs if the wind comes steadily from the same direction throughout the year and if there is not enough sand to cover the entire surface. Barchan dunes move proportionally to the wind velocity and inversely proportionally to their height. They are encountered for instance in Peru [4–7], in Namibia [8] and Morocco [9]. On these dune fields, hundreds of barchans can be found, generally all of the same size. The dunes have heights between 1.5 and 10 m, while their bases are typically 40 to 150 m long and 30 to 100 m wide. The windward or stoss-side of the dune has typical slopes between 8° and 20° and is limited by a sharp edge, called the brink. The brink coincides in many cases with the crest of the dune and separates the slip face from the dune's windward side. Roughly speaking, its section is a parabola-like curve reaching from the tip of one horn to the point of maximum slip face height and back to the tip of the other horn. Despite the fact that for more than 50 years geologists and geographers have been measuring dunes in the field and have obtained data on height, width, length, volume and dune velocity, very little is yet known [10,11] about the exact quantitative shape of barchans. From a mathematical point of view, the barchan dune is a symmetrical object in the wind direction, but in nature there are many factors, like non-steady winds or inclined ground surfaces leading to asymmetrical shapes. Numerical simulations to predict the evolution of barchan dunes and their exact shape have been performed by [12,13].

2. Experimental measurements of a barchan dune

2.1. Dune morphology

Qualitatively the crescent-like shape of the barchan is well known. The first measurements concerning barchan dunes and their morphologic relationships were performed by Coursin [15] in Mauritania and Finkel [4] in the Pampa de La Joya in southern Peru. Hastenrath [5,6] analysed barchans in the same area and revisited the site 20 years later. Additional investigations in the same field were undertaken by Lettau

and Lettau [7]. Slattery [8] measured barchan dunes in Namibia. However, they did not measure the entire shape of the dune, but only the typical lengths. Our own field measurements [14] were performed in a dune field in the Sahara desert, located in southern Morocco (former Spanish Sahara) near the city of Laâyoune.

We define for each horn, the lengths L_a , L_b and the widths W_a , W_b independently, as did Finkel [4]. The orientation of the measuring axis is chosen according to the wind direction, which coincides with the symmetry line for a totally symmetric dune. Furthermore, we introduce the length of the slip face L_s and the length L_0 from the dune toe on the windward side to the brink. Finally, the height of the slip face H is defined at the highest point of the brink, which is the intersection of the brink and the longitudinal centerline of the dune.

The relationship between the width of the horns $W = W_a + W_b$ and the height H of the slip face has been studied many times. An overview can be found by Hesp and Hastings [10]. A linear relationship was found between the height H and the width of the horns W :

$$W = a_W H + b_W. \quad (1)$$

For the management of dune movement the volume V of a dune is one of the most interesting features, apart from the rate of movement v_d . Together they determine the bulk flux Q_b of sand transported by the dunes:

$$Q_b = \rho_{\text{sand}} v_d V. \quad (2)$$

To obtain the total flux Q_t , in addition to the bulk flux the inter-dune-flux Q_i , has to be taken into account:

$$Q_t = Q_b + Q_i. \quad (3)$$

A study of these fluxes has been performed by Sarnthein and Walger [16]. In the following we concentrate on the bulk flux and the dune volume.

According to Oulehri [9], the rate of movement of the dunes in the area of Laâyoune is $32 \text{ m}\cdot\text{yr}^{-1}$ for a dune of 9 m height. The bulk density of the dune sand is $1670 \text{ kg}\cdot\text{m}^{-3}$, on average. Using these data and the calculated volume of $23\,000 \text{ m}^3$ for dune 7, we obtain a flux of $1.2 \text{ Mt}\cdot\text{m}^{-1}\cdot\text{yr}^{-1}$ or $736\,000 \text{ m}^4\cdot\text{yr}^{-1}$. Lettau and Lettau [7] estimated a bulk flux of $20\,550 \text{ m}^4\cdot\text{yr}^{-1}$ for an average barchan of the Pampa de La Joya whose height was 3 m. A large barchan with a height of 5.2 m gave a bulk flux of $60\,000 \text{ m}^4\cdot\text{yr}^{-1}$.

The overall length L of a barchan is the sum of the length L_0 from the windward foot of the dune to its crest, the length of the slip face L_s , and the average of the horn lengths $L_h = (L_a + L_b)/2$:

$$L = L_0 + L_s + \frac{L_a + L_b}{2}. \quad (4)$$

This definition uses four lengths, of which only the length of the slip face L_s has an obvious dependence on the height H :

$$L_s = \frac{H}{\tan \Theta}, \quad (5)$$

where Θ is the angle of repose with typical values between 31° and 35° . This angle is an intrinsic property of the sand and is therefore independent on the aeolian processes.

Finkel [4] reported for the horn length:

$$L_x = a_x H + b_x. \quad (6)$$

Further the ratio of the horn length L_h to the stoss-side length L_0 also depends on the dune height. This shows clearly that the relative position of the slip face within the whole dune varies from small to large

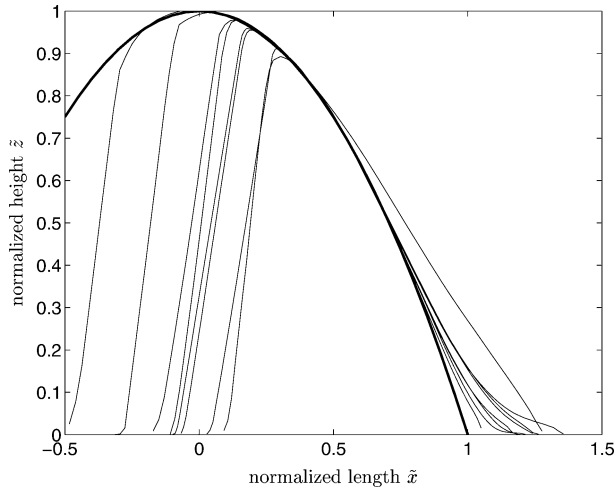


Figure 2. Profile along the symmetry plane of the dunes (thin lines) using normalized variables and the standard parabola (thick line) from [14].

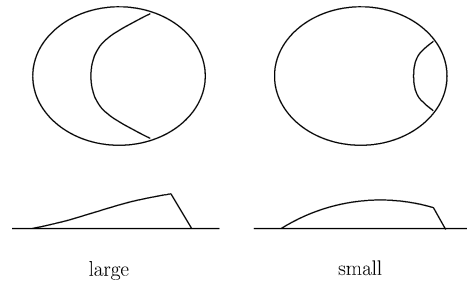


Figure 3. Sketch of a small and a large dune.

dunes and that the ratio of horn length to total length increases with the height as shown in Fig. 3. This disproves scaling invariance of barchan dunes. The size scaling of Barchans can be used to put them all on top of each other by rescaling the axis for each dune and using dimensionless variables. This is done for the longitudinal cross section in Fig. 2. We see that on the windward part the shape is a paraboloid and the brink position b_o moves to the right for larger dunes. In fact b_o is a linear function of the height. Therefore we have a deviation from perfect size scaling as shown in Fig. 3. Looking from the top, the brink line has also the shape of a parabola.

2.2. Wind velocity and sand flux

Correlated measurements of the wind velocity v and the sand flux q have been performed [17] on a large barchan dune near the beach of Jericoacoara (see Fig. 4) during the first week of December 2000, at the end of the dry season. The dune was approximately 34 m in height, a width of 600 m, and the length of its windward side is 200 m.

When a fully turbulent atmospheric boundary layer develops over a flat surface it gives rise to a logarithmic velocity profile $v(z)$ [18],

$$v(z) = \frac{u_*}{\kappa} \ln \frac{z}{z_0}, \tag{7}$$

where u_* denotes the shear velocity, z_0 the roughness length of the surface, and $\kappa = 0.4$ the von Kármán constant. The shear velocity u_* has dimensions of velocity but is defined in terms of the shear stress $\tau = \rho_{\text{air}} u_*^2$ and density ρ_{air} of the air. According to Hunt et al. [19], the height l of the shear stress layer can be obtained implicitly through

$$l = \frac{2\kappa^2 L}{\ln l/z_0}, \tag{8}$$

where L is the characteristic length of the dune which is measured from the half height of the windward side to the crest, according to the definition of [19]. From equation (8), we obtain for $L = 100$ m and a roughness length $z_0 = 10^{-4}$ m, a height of this layer of $l \approx 3.2$ m ($l \approx 4$ m for $z_0 = 10^{-3}$ m). Hence, we placed the anemometers at a height of 1 m, that is, well inside the shear stress layer. One should note that it is very difficult to measure the wind velocity with standard anemometers within this layer for small dunes. This is

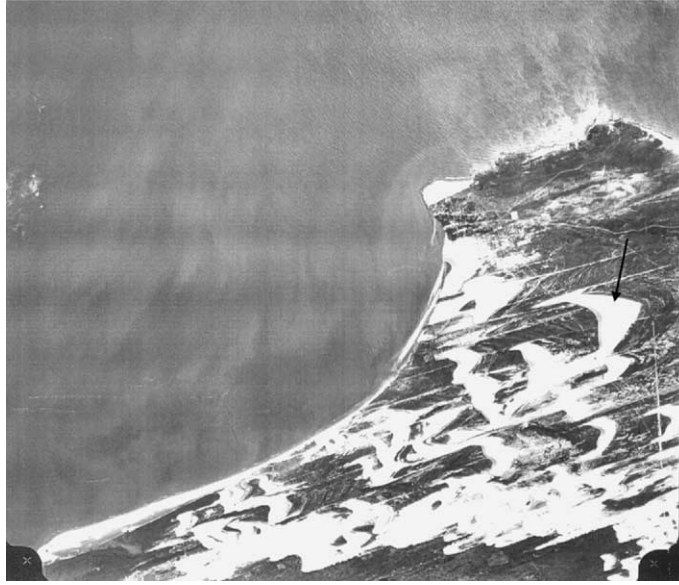


Figure 4. Aerial photography of the coastal dune field near Jericoacoara.

the main reason for choosing a large dune. A reference anemometer has been placed approximately 300 m upwind of the dune foot and has been kept there during all the measurements. With a second anemometer, we measured the average velocity v_i every 24 m on the central profile during 10 minutes. Finally, we normalized the average velocity $\langle v_i \rangle$ by the average velocity in the same period obtained from the reference anemometer, $\langle v_{r,i} \rangle$. By doing so, we could get rid of the long term (> 10 minutes) variations in the wind speed time series throughout the day and obtain the shear velocity $u_{*,i}$ through

$$1 + \hat{u}_{*,i} = \frac{u_{*,i}}{u_{*0}} = \frac{\langle v_i \rangle}{\langle v_{r,i} \rangle}, \quad (9)$$

where $\hat{u}_{*,i}$ is the dimensionless shear velocity perturbation of the air caused by the dune and u_{*0} is the undisturbed shear velocity far upwind of the dune. u_{*0} can be calculated assuming a typical logarithmic profile from turbulent flow equation (7). During our measurements, the wind was blowing quite constantly and had an average value of $7.5 \text{ m}\cdot\text{s}^{-1}$ at the reference station. Assuming a roughness length $z_0 = 2.5 \cdot 10^{-4} \text{ m}$, we obtain from Eq. (7) the undisturbed shear velocity over the plane $u_{*0} = 0.36 \text{ m}\cdot\text{s}^{-1}$. The averaged and normalized measured shear velocities are plotted in Fig. 5.

We also measured the sand flux on the central slice of the dune using cylindrical traps with a diameter of 5 cm and an opening of 1 cm at the front. The back-side of the traps have an opening of 2 cm covered by a fabric with pores smaller than the grain diameter. The traps were placed at the same positions where the wind speed has been measured. From the mass m of the collected sand, the collection time T , and the width w of the opening, we calculated the sand flux $q = m/(Tw)$. The measured sand fluxes are shown in Fig. 6.

3. The model

Since we are interested in the formation and movement of dunes, the important time scale of our problem is defined by the erosion processes that change the surface. A significant change of the surface happens within some hours or even days. In contrast to this, the time scale of the wind and the saltation process

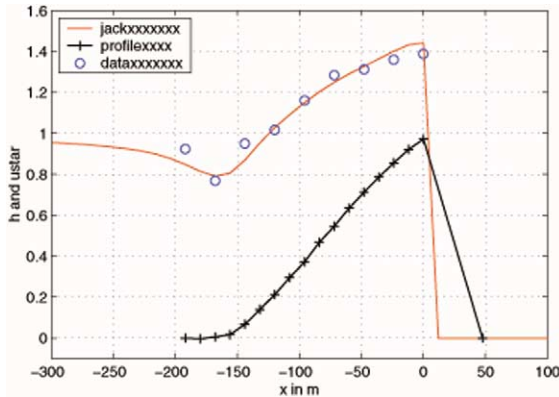


Figure 5. The circles show the measured shear velocity u_* and wind speed $v(z = 1 \text{ m})$ normalized by their reference values u_{*0} and $v_0(z = 1 \text{ m})$, respectively. The solid line depicts the prediction of Eq. (11) using the measured height profile $h(x)$ shown in the bottom curve (crosses). The depression at the dune foot is about 0.8 and the maximum speed-up at the brink is approximately 1.4 from [17].

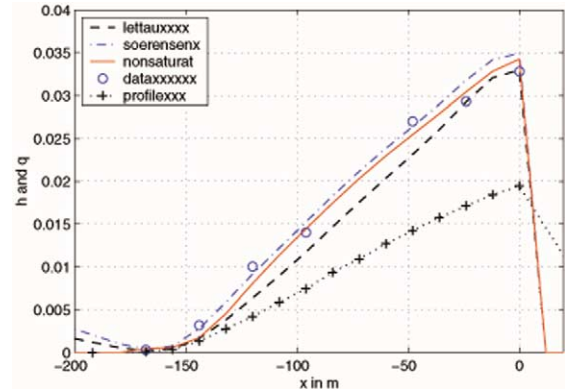


Figure 6. Measured and calculated sand flux onto the central slice of a barchan dune. The circles denote measurements and the solid line the prediction of the non-equilibrium sand flux model, Eq. (13) (solid line). The two dashed lines correspond to the classical empirical relation for saturated flux [19,27]. However, these saturated sand flux relations cannot correctly predict the sand flux near the dune foot and show clearly that the assumption of saturation breaks down from [17].

is in the order of seconds and therefore several orders of magnitude faster. Hence, we will use in the following stationary solutions for the wind field and the sand flux. Similarly we neglect the finite life time of avalanches (a few seconds) and consider them as instantaneous compared to the movement of the dunes. The separation of the different time scales and the resulting approximations lead to an enormous simplification, because it decouples the different physical processes. The entire model can be thought of as four (almost) independent parts: the stationary wind field over a complex terrain, the stationary aeolian sand transport, the time evolution of the surface due to erosion, and avalanches.

3.1. The wind shear stress

The fully turbulent atmospheric boundary layer develops over a flat surface the well-known logarithmic velocity profile $v(z)$ of Eq. (7) [18]. A perturbation of the ground $h(x)$ such as a dune or hill gives rise to a non-local perturbation $\hat{\tau}(x)$ of the undisturbed air shear stress τ_0 :

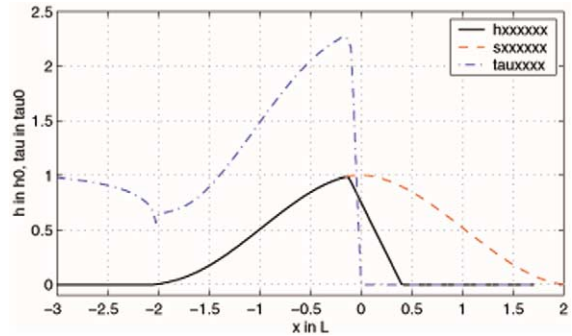
$$\tau(x) = \tau_0 [1 + \hat{\tau}(x)]. \tag{10}$$

The functional dependence of the air shear stress perturbation is crucial for the theoretical understanding of the stability of dunes and to predict the sand flux onto the windward side of a dune. Analytical calculations of the flow over a gentle hill yield an analytical expression for the shear stress perturbation $\hat{\tau}(x)$ [19–21]. We performed further simplifications in order to obtain a minimal expression that captures the crucial features (and only those) and is applicable for sand dunes [22]. The resulting formula for the air shear stress perturbation $\hat{\tau}$ is

$$\hat{\tau}(x) = A \left(\frac{1}{\pi} \int_{-\infty}^{\infty} \frac{h'}{x - \xi} d\xi + Bh' \right), \tag{11}$$

where h' denotes the spatial derivative of the dune's profile $h(x)$ in wind direction. The coefficients $A(L/z_0)$ and $B(L/z_0)$ depend only logarithmically on the ratio between the characteristic length L of the dune and the roughness length z_0 of the surface. For a dune with a length and width ratio $W/L \approx 1$

Figure 7. The envelope $\tilde{h}(x)$ of the windward profile of a dune $h(x)$ and the separating streamline $s(x)$ form together a smooth object which is used to calculate the air shear stress $\tau(x)$ on the windward side. In the region of recirculation the air shear stress τ is set to zero.



and $L/z_0 = 4.0 \cdot 10^5$ we obtain $A \approx 3.2$ and $B \approx 0.3$ from [14,22]. Eq. (11) has several features that are important for dune formation. First, the air shear stress is completely scale invariant and leads to the same speed-up for small and large dunes. This is expected in the fully turbulent regime where no characteristic length exists. Secondly, the shear stress perturbation $\hat{\tau}(x)$, Eq. (11), scales with the height H and inversely with the characteristic length L of the dune and thus with the average slope of the dune windward side, $\hat{\tau} \propto H/L$. Thirdly, a depression of $\tau(x)$ in front of the hill occurs as a consequence of the strongly non-local contribution in Eq. (11). Finally, the shear stress perturbation $\hat{\tau}(x)$ for the windward side of the dune is calculated using Eq. (11), the profile $h(x)$ on the windward side, and the separating streamline $s(x)$ on the lee side. The result is shown in Fig. 5 together with the measured mean values (averages over 10 minutes intervals) normalized according to Eq. (9). The agreement between model results and measurements is good. From this, we can conclude that the heuristic model of the separation bubble combined with the analytic expression, Eq. (11), provide a reasonable approximation for the wind field above the dune. This strategy enormously reduces the computational effort, compared to the numerical solution of turbulence models and the averaged three dimensional Navier–Stokes equation.

Equation (11) is based on a perturbation theory and can only be applied to smooth hills. Jackson and Hunt [20] assumed $H/L < 0.05$, whereas Carruthers et al. [23] showed that mean slopes up to $H/L \approx 0.3$ give reasonable results. The windward side of a barchan dune is always below the latter value and the formula should be applicable. However, flow separation occurs at the brink, which is out of the scope of the linear perturbation theory. A heuristic solution to solve this problem has been suggested by Zeman and Jensen [24]. They introduced a separation bubble that comprises the recirculating flow (the large eddy in the wake of the dune), which reaches from the brink (the point of detachment) to the bottom (to the point of reattachment) see Fig. 7. We model the separating streamline by a third order polynomial that is a smooth continuation of the profile $h(x)$ at the brink x_{brink} and at the reattachment point $x_{\text{brink}} + L_r$, i.e. $h(x_{\text{brink}}) = s(0)$, $h'(x_{\text{brink}}) = s'(0)$, $s(L_r) = 0$, $s'(L_r) = 0$, where $L_r \approx 6H$ is the downwind distance of the reattachment point from the brink. The shear stress perturbation $\hat{\tau}(x)$ for the windward side of the dune is finally calculated using Eq. (10), the profile $h(x)$ on the windward side, and the separating streamline $s(x)$ on the lee side. An example is depicted in Fig. 7.

3.2. The sand flux

Sand transport has been studied already by Bagnold [25] and it was also he who proposed the first phenomenological law that predicted the sand transport from the shear stress of the air. Improved laws have been proposed by several authors in the meantime [7,26,27]. However, all these relations assume that the sand flux q is in equilibrium and can be written as a function of the shear stress τ , $q(\tau(x))$. Temporal or spatial transients are completely neglected. In the following we will call such a relation ‘saturated’, because it predicts the amount of sand that can be maintained in the saltation layer at a certain air shear stress τ .

This condition is hardly fulfilled at the windward foot of an isolated dune [21], e.g. a barchan, where the bed changes rapidly from bedrock or vegetation to sand. Besides the particular conditions at the dune

foot, the sand flux may never reach saturation [28] on the entire windward side, where the shear velocity increases gradually from the foot to the crest. Wind tunnel measurements indicate that the typical time to reach saturation in saltation is approximately two seconds [29], which corresponds to a saturation length of the order of 10 m. This length is of the order of the dune size and can not be neglected if the sand flux on the entire windward side is significant. Furthermore, it has been observed that the time to reach saturation increases for shear velocities close to the threshold [29]. In this situation, the sand flux may never reach saturation on the entire windward side and should increase exponentially with distance from the dune foot [28]. In recent years, several models to calculate the wind field have been developed, from analytic boundary layer approximations to numerical solutions of the Navier–Stokes equation with an enormous computational effort. Although some previous studies have discussed the limits of the saturation approximation in detail [21], much less effort has been dedicated to the development of sand flux relations that effectively incorporate non-saturation effects [30].

For the saturated flux many different functional forms of these sand transport laws exist and have been used in the past. However, for high shear stresses they all converge to the simple relation proposed by [1]:

$$q_s \propto \tau^{3/2}. \quad (12)$$

All other more elaborate relations add higher order corrections to the Bagnold formula that become important close to the air shear stress threshold. To overcome the limitation of saturation and to obtain information about the dynamics of the saltation process, numerical simulations on the grain scale have been performed in the last years [31–33]. Still, concerning the modeling of dune formation, both approaches had to be discarded. The microscopic models are computationally too expensive and the equilibrium assumption that is inherent in the simple flux relations does not hold on the entire windward side of a dune [11,12,14,21,34]. Since both known approaches cannot be used to model dune formation we developed a new phenomenological continuum saltation model that is computationally very efficient on the one side and on the other side incorporates the dynamics of the saltation layer and thus allows for saturation transients [34]. In this model the sand flux is defined by a differential equation of the form

$$\frac{\partial}{\partial x} q = \frac{1}{l_s} q \left(1 - \frac{q}{q_s} \right), \quad (13)$$

where $q_s(\tau)$ is the saturated sand flux and $l_s(\tau)$ the characteristic length of the saturation transients, called saturation length. The saturation length $l_s(\tau)$ depends on the air shear stress, but converges towards a constant value for $\tau \gg \tau_t$ [34]. A comparison between the saturated sand flux and our model, Eq. (13), calculated on cosine shaped hills of different size, can be seen in Fig. 6.

3.3. The surface evolution

A spatial change in sand flux implies that erosion or deposition takes place and the surface changes in height. The time evolution of the surface can be calculated from the conservation of mass:

$$\frac{\partial h}{\partial t} = \frac{1}{\rho_{\text{sand}}} \frac{\partial q}{\partial x}, \quad (14)$$

where ρ_{sand} is the bulk density of dune sand. Finally, we note that Eq. (14) is the only remaining time dependent equation and thus defines the time scale of the model.

The full dune model can be sketched as follows. An initial surface h is used to start the time evolution. If flow separation has to be modeled the separating streamline $s(x)$ is calculated. Next, the air shear stress $\tau(x)$ onto the given surface h (or h and s) is calculated using Eq. (10). From the air shear stress $\tau(x)$ the sand flux can be determined using Eq. (13). Then, the integration forward in time of the surface is calculated

from the mass conservation, Eq. (14). Finally, sand is eroded and transported downhill if the local angle $\partial_x h$ exceeds the angle of repose. This redistribution of mass (avalanches) is performed until the surface slope has relaxed below the critical angle. The time integration is calculated until the final shape invariantly moving solution is obtained.

4. The shape of the dune and outlook

In order to analyze the properties of the shape-invariantly moving solution of our model, we performed a series of calculations varying the volumes of the Gaussian hills that have been used as initial configuration. The final shape invariantly moving solutions are displayed in Fig. 8. For small volumes we obtained heaps without a slip face, whereas for large volumes dunes with a slip face developed. Hence, there is a minimal height for dune formation or, more precisely, a minimal height for the formation of a slip face. Empirically, this was observed many times in nature. Also, rescaling the dunes by their heights gives the behaviour shown in Fig. 2.

The simulation also showed that the barchan shape is a steady state solution. Starting from different initial configurations having the same volume, one always obtains after a certain transient the same crescent shape dune. This dune moves with constant velocity which quantitatively agrees with the ones measured in the field for corresponding volume.

One can also using our programme construct virtual dunes and produce virtual desert landscapes. One example is shown in Fig. 9 where one sees the resulting coalescence of barchans after they have developed from a set of several Gaussian heaps. In this way one can, starting from measured topographies predict the future evolution and therefore planify in advance to protect cities and fields against moving sand masses in the Sahara. Another perspective of the use of our equations of motion is the possibility to study techniques used to stop or destroy dunes, like Bofix, as introduced by Meunier in Nouakchott.

Acknowledgements. I want to thank my collaborators P. Rognon, J.S. de Andrade, A. Poliakov, L. Parente and K. Kroy and in particular Gerd Sauermaann whose thesis work has largely been reviewed here.

Figure 8. The solutions for large volumes—above a critical height—are dunes including a slip face, whereas for small volumes heaps develop. An important fact is that the steepest lee side of a heap (dashed lines) is approximately 15° , which is well below the angle of repose of 34° .

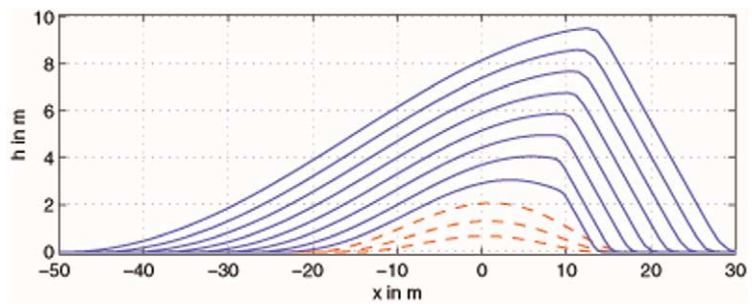
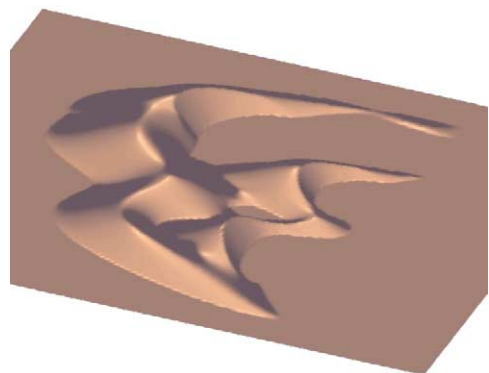


Figure 9. Complex dune pattern, calculated with the full three-dimensional model. Wind is blowing from the left to the right. When barchan dunes are too close they interact, get eventually connected, and form complex dune structures. The large dunes are shielding the small dunes from the arriving sand flux which then constantly loose volume [35].



References

- [1] R.A. Bagnold, *The Physics of Blown Sand and Desert Dunes*, Methuen, London, 1941.
- [2] K. Pye, H. Tsoar, *Aeolian Sand and Sand Dunes*, Unwin Hyman, London, 1990.
- [3] N. Lancaster, *Geomorphology of Desert Dunes*, Routledge, London, 1995.
- [4] H.J. Finkel, The Barchans of Southern Peru, *J. Geol.* 67 (1959) 614–647.
- [5] S. Hastenrath, *The Barchans of the Arequipa Region, Southern Peru*, 1967.
- [6] S. Hastenrath, The barchan dunes of Southern Peru revisited, *Z. Geomorph.* 31 (2) (1987) 167–178.
- [7] K. Lettau, H. Lettau, Bulk transport of sand by the barchans of the Pampa de La Joya in Southern Peru, *Z. Geomorph. NF* 13 (2) (1969) 182–195.
- [8] M.C. Slattery, Barchan migration on the Kuiseb river delta, Namibia, *South African Geogr. J.* 72 (1990) 5–10.
- [9] T. Oulehri, *Étude géodynamique des migrations de sables éoliens dans la région de Laâyoune (Nord du Sahara marocain)*, PhD thesis, l'Université Paris 6, no. 92-12, Paris, 1992.
- [10] P.A. Hesp, K. Hastings, Width, Height and slope relationships and aerodynamic maintenance of barchans, *Geomorphology* 22 (1998) 193–204.
- [11] G.F.S. Wiggs, I. Livingstone, A. Warren, The role of streamline curvature in sand dune dynamics: evidence from field and wind tunnel measurements, *Geomorphology* 17 (1996) 29–46.
- [12] F.K. Wippermann, G. Gross, The wind-induced shaping and migration of an isolated dune: A numerical experiment, *Bound. Layer Meteor.* 36 (1986) 319–334.
- [13] A.D. Howard, J.B. Morton, Sand transport model of barchan dune equilibrium, *Sedimentology* 25 (1978) 307–338.
- [14] G. Sauer mann, P. Rognon, A. Poliakov, H.J. Herrmann, The shape of the barchan dunes of Southern Morocco, *Geomorphology* 36 (2001) 47–62.
- [15] A. Coursin, Observations et expériences faites en avril et mai 1956 sur les barkhans du Souehel el Abiodh (région est de Port-Étienne), *Bull. IFAN* 22A (3) (1964) 989–1022.
- [16] M. Sarnthein, E. Walger, Der äolische Sandstrom aus der W-Sahara zur Atlantikküste, *Geolog. Rund.* 63 (1974) 1065–1087.
- [17] G. Sauer mann, L.P. Andrade Jr., J.S. Maia, U.M.S. Costa, A.D. Araújo, H.J. Herrmann, Wind Velocity and Sand Transport on a Barchan Dune, 2001.
- [18] O. Landau, O. Lifshitz, *Fluid Mechanics, Course of Theoretical Physics*, Vol. 6, Pergamon Press, London, 1963.
- [19] J.C.R. Hunt, S. Leibovich, K.J. Richards, Turbulent wind flow over smooth hills, *Quart. J. Roy. Meteorol. Soc.* 114 (1988) 1435–1470.
- [20] P.S. Jackson, J.C.R. Hunt, Turbulent wind flow over a low hill, *Quart. J. Roy. Meteorol. Soc.* 101 (1975) 929.
- [21] W.S. Weng, J.C.R. Hunt, D.J. Carruthers, A. Warren, G.F.S. Wiggs, I. Livingstone, I. Castro, An experimental study of Froude number effect on wind-tunnel saltation, *Acta Mech. Suppl.* 1 (1991) 145–157.
- [22] K. Kroy, G. Sauer mann, H.J. Herrmann, A minimal model for sand dunes, *Phys. Rev. Lett.* 88 (2002) 054301.
- [23] D.J. Carruthers, J.C.R. Hunt, *Fluid Mechanics of Airflow over Hills: Turbulence, Fluxes, and Waves in the Boundary Layer*, Chapter Atmospheric Processes over Complex Terrain, Vol. 23, Amer. Meteorol. Society, 1990.
- [24] O. Zeman, N.O. Jensen, Progress report on modeling permanent form sand dunes, Risø National Laboratory, M-2738, 1988.
- [25] R.A. Bagnold, The movement of desert sand, *Proc. R. Soc. London Ser. A* 157 (1936) 594–620.
- [26] P.R. Owen, Saltation of uniformed sand grains in air, *J. Fluid. Mech.* 20 (1964) 225–242.
- [27] M. Sørensen, An analytic model of wind-blown sand transport, *Acta Mech. (Suppl.)* 1 (1991) 67–81.
- [28] N. Lancaster, W.G. Nickling, C.K. McKenna Neumann, V.E. Wyatt, Sediment flux and airflow on the stoss slope of a barchan dune, *Geomorphology* 17 (1996) 55–62.
- [29] G.R. Butterfield, Sand transport response to fluctuating wind velocity, Chapter 13, in: N.J. Clifford, J.R. French, J. Hardisty (Eds.), *Turbulence: Perspectives on Flow and Sediment Transport*, Wiley, 1993, pp. 305–335.
- [30] P.M. van Dijk, S.M. Arens, J.H. van Boxel, Aeolian processes across transverse dunes ii: Modelling the sediment transport and profile development, *Earth Surf. Process. Landforms* 24 (1999) 319–333.
- [31] S. Anderson Robert, K. Haff Peter, Simulation of eolian saltation, *Science* 241 (1988) 820.
- [32] R.S. Anderson, Wind modification and bed response during saltation of sand in air, *Acta Mech. (Suppl.)* 1 (1991) 21–51.
- [33] I.K. McEwan, B.B. Willetts, Numerical model of the saltation cloud, *Acta Mech. (Suppl.)* 1 (1991) 53–66.
- [34] G. Sauer mann, K. Kroy, H.J. Herrmann, A phenomenological dynamic saltation model for dune formation, *Phys. Rev. E* 64 (2001) 31305.
- [35] G. Sauer mann, Modeling of wind blown sand and desert dunes, PhD thesis, Universität Stuttgart, 2001.
- [36] B.R. White, H. Mounla, An experimental study of Froude number effect on wind-tunnel saltation, *Acta Mech. Suppl.* 1 (1991) 145–157.